
MOLECULAR PROPERTY PREDICTION BY SEMANTIC-INVARIANT CONTRASTIVE LEARNING

Ziqiao Zhang
Fudan University
Shanghai
zqzhang18@fudan.edu.cn

Ailin Xie
Fudan University
Shanghai
alxie21@m.fudan.edu.cn

Jihong Guan
Tongji University
Shanghai
jhguan@tongji.edu.cn

Shuigeng Zhou*
Fudan University
Shanghai
sgzhou@fudan.edu.cn

ABSTRACT

Contrastive learning have been widely used as pretext tasks for self-supervised pre-trained molecular representation learning models in AI-aided drug design and discovery. However, exiting methods that generate molecular views by noise-adding operations for contrastive learning may face the semantic inconsistency problem, which leads to false positive pairs and consequently poor prediction performance. To address this problem, in this paper we first propose a semantic-invariant view generation method by properly breaking molecular graphs into fragment pairs. Then, we develop a Fragment-based Semantic-Invariant Contrastive Learning (FraSICL) model based on this view generation method for molecular property prediction. The FraSICL model consists of two branches to generate representations of views for contrastive learning, meanwhile a multi-view fusion and an auxiliary similarity loss are introduced to make better use of the information contained in different fragment-pair views. Extensive experiments on various benchmark datasets show that with the least number of pre-training samples, FraSICL can achieve state-of-the-art performance, compared with major existing counterpart models.

Keywords Molecular representation learning · Molecular property prediction · Contrastive learning

1 Introduction

Nowadays molecular property prediction (MPP) based on deep learning techniques has been a hot research topic of the AI-aided Drug Discovery (AIDD) community [1, 2, 3, 4, 5, 6, 7]. As most of the molecular properties that drug discovery studies concern require *in vivo* or *in vitro* wet-lab experiments to measure, labeled data for MPP tasks are typically scarce, because it is expensive and time-consuming to acquire such data [8]. On the contrary, there are large amounts of public available unlabeled data [9, 10, 11]. Therefore, how to use these large-scale unlabeled molecular data to train deep neural networks to learn better molecular representations for MPP tasks, is of great interest to the AIDD community.

Recently, as self-supervised pre-trained models (e.g. BERT [12], MoCo [13] and SimCLR [14]) have shown significant superiority in the fields of Natural Language Processing (NLP) and Computer Vision (CV), self-supervised learning (SSL) has become a mainstream method of utilizing large-scale unlabeled molecular data in MPP study. These SSL methods typically use some inherent features within or between samples to construct pretext tasks, so that unlabeled data can be leveraged to train deep models in a self-supervised learning manner [15]. Contrastive learning, masked language model and predictive learning are the currently three categories of methods to design pretext tasks in MPP studies [16, 17, 18, 19, 20, 21, 22, 23]. Inspired by SimCLR, contrastive learning methods aim at learning representations through contrasting positive data pairs against negative ones [16]. Original molecular structures are

augmented into multiple views, and views generated from the same molecule are typically used as positive data pairs, while views of different molecules are taken as negative ones [16].

The way to generate molecular views is crucial to the design of contrastive learning pretext tasks for molecular representation learning. As a kind of special objects, molecules can be represented by different methods, including molecular fingerprints [24], SMILES [25], IUPAC [26], and molecular graph. These different molecular representation methods therefore can naturally be leveraged to generate views for contrastive learning. For instance, the DMP [17] and MEMO [18] models are designed in this way. Following the practice in CV, another widely used category of methods tries to *add noise* into molecular structures to generate transformations of the original molecules. These noise-adding operations include deleting atoms, replacing atoms, deleting bonds, deleting subgraph structures etc. MolCLR [16] and GraphLoG [21] are such representative models.

Although the noise-adding methods for view generation have been widely used in CV studies [14, 27], when applying these methods into MPP tasks, a fact that has not been noticed by the researchers is that molecules are very sensitive to noise. Arbitrarily modifying the topological structure of a molecule with noise, the generated new structure may represent a totally different molecule. For instance, as shown in Fig. 1(a), adding noise into an dog image by randomly masking some area will not change the semantic of the generated view, which is still a yellow dog. However, in Fig. 1(b), for an acetophenone molecule, deleting a subgraph leads to a benzene molecule, indicating that acetophenone’s chemical semantic is completely changed. And small modification to molecular structure can lead to dramatic changes in the properties of modified molecules, including both bio-activity and other physio-chemical properties. Concretely, from the PubChem database we can find that the LogP value of acetophenone in Fig. 1(b) is 1.58, while that of benzene is 2.13. The difference is almost 35%. Therefore, it is unreasonable to treat these two views (molecules) as a positive pair for contrastive learning.

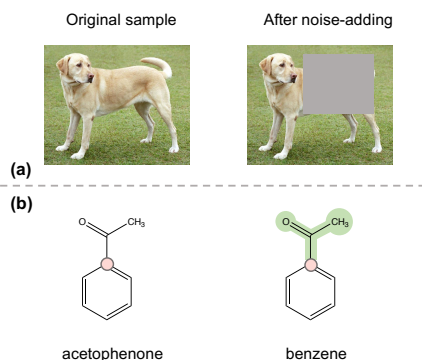


Figure 1: Illustration of the influence of noise-adding operation to the semantic of generated view. (a) After adding noise to the image by randomly masking some area, the semantic of dog image does not change, i.e., the image still represents a dog. (b) By adding noise into the molecular structure by masking some atoms and edges, the molecule *acetophenone* becomes a completely different molecule *benzene* with different molecular properties. That is, the chemical semantic of *acetophenone* is completely changed.

Aiming at solving this semantic inconsistency problem, this paper proposes a **F**ragment-based **S**emantic-**I**nvariant **C**ontrastive **L**earning molecular representation model, named FraSICL. A semantic-invariant molecular view generation method is developed, in which a molecular graph is properly broken into fragments by changing the message passing topology while preserving the topological information. A multi-view fusion mechanism is introduced to FraSICL to make better use of the information contained in views of different fragments and avoid the impact of randomness. In addition, an auxiliary similarity loss is designed to train the backbone Graph Neural Network (GNN) to generate better representation vectors.

Our contribution are summarized as follows:

- We raise the semantic inconsistency problem in molecular view construction for molecular contrastive learning and develop an effective method to generate semantic-invariant graph views by changing message passing topology while preserving the topological information.
- We propose a novel Fragment-based Semantic-Invariant Contrastive Learning molecular representation model for effective molecular property prediction, which is also equipped with a multi-view fusion mechanism and an auxiliary similarity loss to better leverage the information contained in unlabeled pre-training data.

- Extensive experiments show that compared with SOTA pre-trained molecular property prediction models, the proposed FraSICL can achieve better prediction accuracy on downstream target tasks with less amounts of unlabeled pre-training data.

2 Method

Here, we first formally define semantic-invariant molecular view in Sec. 2.1, then propose a semantic-invariant molecular view generation method in Sec. 2.2 and a multi-view fusion scheme in Sec. 2.3. Finally, we present the structure of the Fragment-based Semantic-Invariant Contrastive Learning (FraSICL) molecular representation model in Sec. 2.4 and its loss functions in Sec. 2.5.

2.1 Semantic-invariant Molecular View

In Sec. 1, we give an example to illustrate how noise-adding operations may lead to semantic inconsistency and consequently false positive pairs. Here, we will formally define *semantic-invariant molecular view*.

Given a molecule m and its molecular graph $G = \{V, E, X_{atom}, X_{bond}\}$ (hydrogen-depleted) where V denotes the set of nodes that represent the atoms, E denotes the set of edges between nodes, representing the bonds. X_{atom} and X_{bond} are feature matrix of atoms and bonds respectively. A *transformation function* $F(\cdot)$ is used to generate a *molecular graph view* (or simply *molecular view*) G' of G , i.e., $G'=F(G)$ and $G'=\{V', E', X'_{atom}, X'_{bond}\}$. In what follows, we first define two types of semantic inconsistent views.

Definition 1 (Semantic-conflict view) *If there is another molecule m_2 whose molecular graph is G_2 , and $G_2=G'=F(G)$, i.e., the view G' of m is the same as the molecular graph G_2 of m_2 , then we say G' is a semantic-conflict view of m with regard to (w.r.t.) m_2 .*

Definition 2 (Semantic-ambiguity view) *If there exists another molecule m_2 whose molecular graph is G_2 , and $G'_2=F(G_2)=G'=F(G)$, i.e., the view G' of m is the same as a view G'_2 of m_2 . Then, we say G' is a semantic-ambiguity view of molecule m w.r.t. molecule m_2 .*

Both semantic-conflict views and semantic-ambiguity views will lead to false positive pairs for molecular representation contrastive learning. For example, assume that a Graph Neural Network $g(\cdot)$ serves as an encoder to embed the molecular graphs into latent graph embeddings $\mathbf{h}_G = g(G)$. If we ignore the randomness in the encoder, it is obvious that, for molecule m , if it has a semantic-conflict view w.r.t. molecule m_2 , i.e., $G'=F(G)=G_2$, then the representation of G' embedded by the graph neural network will be the same as that of G_2 . That is, $\mathbf{h}_{G'}=g(G')=\mathbf{h}_{G_2}=g(G_2)$. In this case, as \mathbf{h}_G and $\mathbf{h}_{G'}$ are considered as a positive pair in contrastive learning, \mathbf{h}_G and \mathbf{h}_{G_2} are consequently used as a positive pair. In another word, the contrastive loss will implicitly make the representations of molecule m and m_2 to be close. However, as claimed before, the molecular properties of different molecules may be greatly different, so that they cannot be used as a positive pair for contrastive learning. Therefore, semantic-conflict views will lead to false positive pairs and degrade learning performance.

On the other hand, if a semantic-ambiguity view is generated as defined in Def. 2, i.e., $F(G_2)=G'=F(G)$, indicating that the contrastive loss will make \mathbf{h}_G and $\mathbf{h}_{G'}$, \mathbf{h}_{G_2} and $\mathbf{h}_{G'}$ to be close in the embedding space, thus \mathbf{h}_G and \mathbf{h}_{G_2} to be close too. That is, the representations of molecules m and m_2 are consequently close by contrastive learning. So semantic-ambiguity views will also lead to false positive pairs.

To boost the performance of contrastive learning for MPP, we should avoid the generation of both semantic-conflict views and semantic-ambiguity views. That is, we generate only semantic-invariant views, which are defined as follows:

Definition 3 (Semantic-invariant view) *Given a view G' of molecule m with graph G , if G' is neither a semantic-conflict view nor a semantic-ambiguity view w.r.t. any other molecules, then we say G' is a semantic-invariant view of m .*

In next section, we will give a method to generate semantic-invariant views.

2.2 Semantic-invariant View Generation

According to Def. 3 in Sec. 2.1, semantic-invariant views should be neither semantic-conflict views nor semantic-ambiguity views. Besides, from the perspective of prediction, they should also be discriminative. That is, they can be encoded into different representations by neural network encoders. In this section, to achieve these goals, we propose a semantic-invariant view generation method.

Table 1: Properties of atoms and bonds in X_{atom} and X_{bond} .

Indices of atomic features	Description
0-15	Atomic symbol, a one-hot vector of [B,C,N,O,F,Si,P,S,Cl,As,Se,Br,Te,I,At,metal]
16-21	Number of bonds
22	Electrical charge
23	Number of radical electrons
24-29	Hybridization, a one-hot vector of [sp, sp ² , sp ³ , sp ³ d, sp ³ d ² , other]
30	Aromaticity
31-35	Number of connected hydrogens
36	Whether the atom is a chiral center
37-38	Chirality type, a one-hot vector of [R,S]
Indices of bond features	Description
0-3	Bond type, a one-hot vector of [single, double, triple, aromatic]
4	Whether the bond is conjugated
5	Whether the bond is in a ring
6-9	Stereo, a one-hot vector of [StereoNone, StereoAny, StereoZ, StereoE]

In our previous study [6], to better capture the hierarchical structural information of molecules, a chemical-interpretable molecule fragmentation method FraGAT is proposed. By considering acyclic single bonds as boundaries between functional groups, the FraGAT model proposes to randomly breaking one of the acyclic single bonds to generate two graph fragments corresponding to some chemical meaningful functional groups. The experimental results show that learning representations by chemical meaningful molecular graph fragments can achieve good predictive performance for MPP tasks. Inspired by these findings, our semantic-invariant view generation method is designed as follows:

Given a molecule m , its molecular graph can be denoted as an annotated graph $G = \{V, E, X_{atom}, X_{bond}\}$. The atom feature matrix X_{atom} and the bond feature matrix X_{bond} are computed according to Tab. 1. Then, remove one of the acyclic single bonds e_{ij} from E , we obtain $G' = \{V, E', X_{atom}, X_{bond}\}$ where $E' = E - \{e_{ij}\}$. We accept G' as a view to be generated, i.e., a semantic-invariant view. As the graph G' consists of two disconnected molecular graph fragments, it is also called *fragment-pair view*.

From the discrimination perspective, G' is a different graph from the original molecular graph G , so that it will make GNN encoders to generate a different representation. Furthermore, as all the acyclic single bonds in a molecule are unique, breaking different acyclic single bonds will lead to different fragment-pair views, whose representations after a GNN encoder will also be different. That is, the generated views for a molecule are discriminative.

Then, is G' a real semantic-invariant view of molecule m according to Def. 3? Let us check.

On the one hand, as the atom feature matrix X_{atom} is not modified, the numbers of bonds of the two vertex i and j of the broken bond e_{ij} encoded in the atom feature vectors of the generated G' remain the same as that in the original molecular graph G . However, the modified E' indicates that there is no edge between i and j , so that the numbers of bonds encoded in the atom feature vectors are not consistent with that in the topological structure. The degrees of node i and j in graph G' are lower than the numbers of bonds of i and j encoded in X_{atom} . In another word, G' is not a valid molecular graph of any molecule. Furthermore, from the graph perspective, because G' consists of two disconnected subgraphs, and no any valid molecule corresponds to a disconnected graph. Therefore, G' cannot be a semantic-conflict view w.r.t. any molecule according to Def. 1.

On the other hand, since only one single bond is removed in view G' , this discrepancy can only be discovered at nodes i and j , and the numbers of bonds of i and j encoded in X_{atom} must be only 1 larger than the degrees of i and j , so the removed edge can only be between i and j , and the removed edge can only be a single bond. Thus, there is no other molecular graph G_2 that can generate the same G' . Similarly, from graph perspective, the graph G of molecule m cannot be equal to the disconnected graph of any view generated from any other molecule. In summary, G' cannot be a semantic-ambiguity view w.r.t. any molecule according to Def. 2.

Finally, from the perspective of graph rewiring [28, 29, 30], the topological information about the broken edge is encoded in the atom feature matrix X_{atom} . So our method preserves the topological structural information of the original molecular graph, but propagates message between nodes through a different topology. Thus, it realizes local decoupling of the input graph topology and the message passing topology. Moreover, compared with randomly breaking

any edges in the molecular graph, our method can generate chemical meaningful graph fragments to benefit the prediction of molecular properties, which has been demonstrated in the experiments of previous work [6].

In conclusion, our method is expected to generate better positive pairs, which will help to train neural networks to generate better molecular representations by contrastive learning.

2.3 Multi-view Fusion

The number of acyclic single bonds of an organic molecule is often large, so there are various fragment-pair views can be generated from one molecule by our proposed view generation method. As demonstrated in the experiments of some existing work [6], different fragment pairs contain different information about functional groups that constitute a molecule, which shows different predictive performance. So, to ensure that the information of the functional groups that determine molecular properties and are contained in the fragment pairs can be obtained by the neural network, in FraSICL, we no longer randomly generate *fragment-pair views* as other contrastive learning models do. Instead, a multi-view fusion mechanism is introduced as follows: Given a molecule with N_b breakable acyclic single bonds, all of the N_b fragment-pair views are generated and the representations of these fragment-pair views are calculated by a GNN encoder. Then, a Transformer encoder is exploited to fuse these representations by the multi-head attention (MHA) mechanism to produce a representation vector that contains information of all of the fragment pairs, named *fragment view*. The details of fragment-pair view fusion are delayed to the next section. The fragment view and the molecule view (i.e., the original molecular graph) are used as two views of a molecule for contrastive learning.

2.4 Model Structure

The structure of the FraSICL model is shown in Fig. 2. Given a molecule m with molecular graph $G_{mol} = \{V, E, X_{atom}, X_{bond}\}$, the model computes the representations of two views via two branches: the left branch is the *molecule view branch* for generating molecular view, and the right one is the *fragment view branch* for generating the fragment view.

In the molecule view branch, a GNN $g_{mol}(\cdot)$ is used as an encoder to capture the representation of the molecular graph $\mathbf{h}_{mol} = g_{mol}(G_{mol})$. Attentive FP [5] is employed as the graph encoder in this work. Then, following the structure of MolCLR [16], \mathbf{h}_{mol} is fed to a projection head $l_{mol}(\cdot)$ and a regularization function $norm(\cdot)$ to produce the projection of the molecule view $\mathbf{p}_{mol} = norm(l_{mol}(\mathbf{h}_{mol}))$. The structure of a projection head is shown in Fig. 3. And the regularization function is $norm(\mathbf{v}) = \frac{\mathbf{v}}{\|\mathbf{v}\|}$, which can make the length of the projection vector be 1.

And for the fragment view branch on the right, all of the N_b breakable acyclic single bonds are enumerated and broken by the method proposed in Sec. 2.2 to generate N_b fragment-pair views $G_{frag}^1 = \{V, E_1, X_{atom}, X_{bond}\}, \dots, G_{frag}^{N_b} = \{V, E_{N_b}, X_{atom}, X_{bond}\}$. Then, a GNN $g_{frag}(\cdot)$ is used as an encoder to compute the representation of each fragment-pair view $\mathbf{h}_{frag}^i = g_{frag}(G_{frag}^i)$. Attentive FP is also used here. Note that since there are two disconnected components in each fragment-pair view G_{frag}^i , $g_{frag}(\cdot)$ will read out these two subgraphs separately and produce two subgraph embeddings. The representation of a fragment-pair view is obtained by element-wisely adding its two corresponding subgraph embeddings for permutation-invariant property.

Then, as described in Sec. 2.3, a multi-view fusion mechanism is introduced for leveraging all of the information related to functional groups contained in the N_b fragment-pair views. Specifically, a Transformer encoder $T(\cdot)$ is employed, which uses the representations of fragment-pair views \mathbf{h}_{frag}^i as input tokens, and computes the interaction relationships between the fragment-pair views by the multi-head attention (MHA) mechanism. The resulting attention scores serve as weights to fuse the representations and obtain $\hat{\mathbf{h}}_{frag}^i$. By summing up all of the representations of N_b *fragment-pair views*, we can get the representation of *fragment view* $\mathbf{h}_{fv} = \sum_{i=1}^{N_b} \hat{\mathbf{h}}_{frag}^i$. Finally, the representation \mathbf{h}_{fv} of the fragment view goes through a projection head $l_{fv}(\cdot)$ and a normalization layer to get $\mathbf{p}_{fv} = norm(l_{fv}(\mathbf{h}_{fv}))$. Following the structure of MolCLR, the two projections \mathbf{p}_{mol} and \mathbf{p}_{fv} are used to calculate contrastive loss. And when finetuning on the downstream tasks, the model will output one of the representations \mathbf{h}_{mol} or \mathbf{h}_{fv} of a molecule to serve as learned molecular representation. A downstream prediction head $f(\cdot)$ will use this representation as input, and predict the molecular property by $y = f(\mathbf{h}_{mol})$ or $y = f(\mathbf{h}_{fv})$.

In addition, representations \mathbf{h}_{frag}^i of N_b fragment-pair views of a molecule goes through another projection head and a normalization layer to produce projection $\mathbf{p}_{frag}^i = norm(l_{frag}(\mathbf{h}_{frag}^i))$. Inner product of these projections are computed to generate a similarity matrix $S = \{s_{ij} | s_{ij} = \langle \mathbf{p}_{frag}^i, \mathbf{p}_{frag}^j \rangle\}$, $S \in \mathbb{R}^{N_b \times N_b}$, where $\langle \cdot, \cdot \rangle$ denotes the inner product of two vectors. The usage of this similarity matrix S will be introduced in the next section.

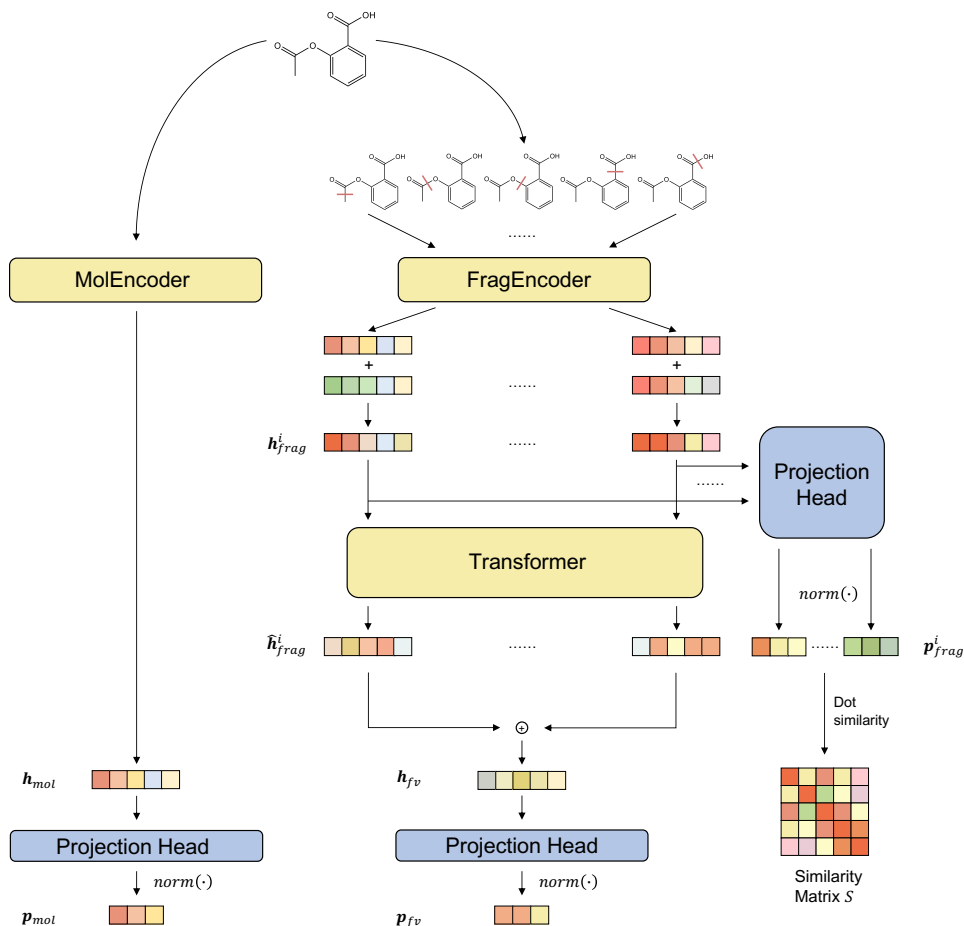


Figure 2: The structure of the FraSICL model.

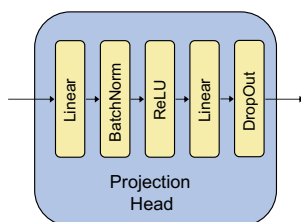


Figure 3: The structure of a projection head. Following the design proposed in BYOL [27], a projection head consists of a stack of linear layer, BN layer, activation layer, linear layer and dropout layer.

2.5 Loss Functions

The training of FraSICL in the pre-training phase is illustrated in Fig. 4. Here, given a batch of N molecules, the model will calculate the projections \mathbf{p}_{mol} and \mathbf{p}_{fv} of each molecule. Then, contrastive learning is performed between all samples in a batch. The view pair (i.e. molecule view and fragment view) of each sample is a positive pair, as shown by the red line, and the view pairs of other samples in the batch are negative pairs, as shown by the blue line in the figure. The NT-Xent Loss is used for contrastive learning:

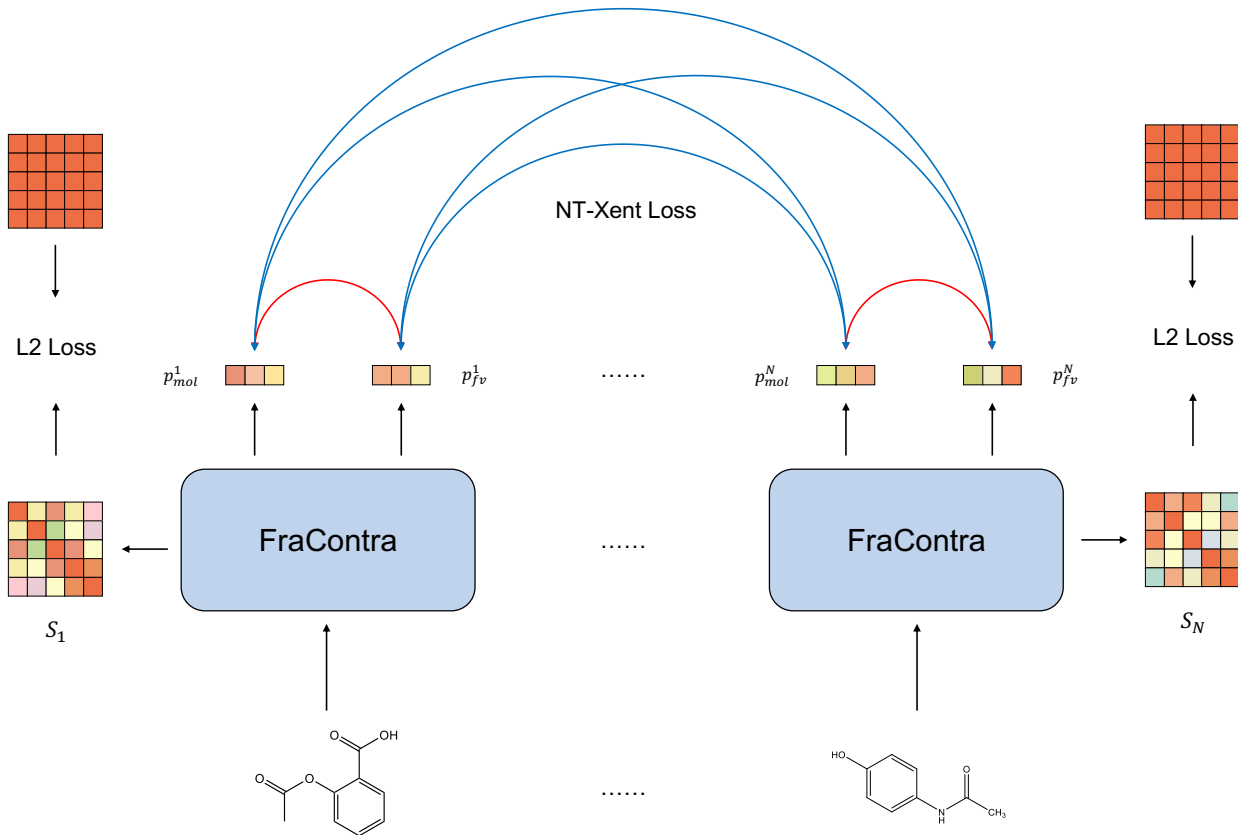


Figure 4: The illustration of FraSICL training. FraSICL is trained by both NT-Xent contrastive loss and an auxiliary similarity loss. In the contrastive loss, two projections of a molecule are treated as a positive pair, which is highlighted by red lines in the figure. Projections of other molecules in a batch are considered as negative pairs, which is shown by blue lines. For each molecule, L2 loss is computed between the similarity S and an all-one matrix as auxiliary similarity loss.

$$\mathcal{L}_{mol}^i = \log \frac{e\left(\frac{sim(\mathbf{p}_{mol}^i, \mathbf{p}_{fv}^i)}{\tau}\right)}{\sum_{k=1}^N \mathbb{1}\{k \neq i\} \left(e\left(\frac{sim(\mathbf{p}_{mol}^i, \mathbf{p}_{mol}^k)}{\tau}\right) + e\left(\frac{sim(\mathbf{p}_{mol}^i, \mathbf{p}_{fv}^k)}{\tau}\right) \right)}, \quad (1)$$

$$\mathcal{L}_{fv}^i = \log \frac{e\left(\frac{sim(\mathbf{p}_{mol}^i, \mathbf{p}_{fv}^i)}{\tau}\right)}{\sum_{k=1}^N \mathbb{1}\{k \neq i\} \left(e\left(\frac{sim(\mathbf{p}_{fv}^i, \mathbf{p}_{mol}^k)}{\tau}\right) + e\left(\frac{sim(\mathbf{p}_{fv}^i, \mathbf{p}_{fv}^k)}{\tau}\right) \right)}, \quad (2)$$

where inner product similarity is adopted for $sim(\mathbf{p}_{mol}^i, \mathbf{p}_{fv}^i)$, and τ is a temperature parameter. The sum of all contrastive losses of a batch of molecules is denoted as $\mathcal{L}_{clr} = \sum_{i=1}^N \mathcal{L}_{mol}^i + \sum_{i=1}^N \mathcal{L}_{fv}^i$.

In addition, although the representations of different fragment-pair views have been fused, from the perspective of contrastive learning, the representations of different fragment-pair views of the same molecule should also be as close as possible. And as demonstrated in previous study [6], representations of some fragment pairs of a molecule are highly predictive on the downstream tasks, while some others are less effective. So, we hope that the representations of fragment-pair views can use information from each other to train the GNN encoder to extract better representations. To this end, an additional auxiliary loss \mathcal{L}_{sim} is introduced to improve the similarity between representations of fragment-pair views of a molecule, based on the similarity matrix S . Since the inner product of two normalized vectors is equivalent to cosine similarity, and the maximum value of cosine similarity is 1, assuming a molecule k have N_b^k

fragment-view pairs, the elements of the similarity matrix are $s_{ij}^k = \langle \mathbf{p}_{frag}^{k,i}, \mathbf{p}_{frag}^{k,j} \rangle$, our auxiliary similarity loss of molecule k is:

$$\mathcal{L}_{sim}^k = \frac{1}{(N_b^k)^2} \sum_{i=1}^{N_b^k} \sum_{j=1}^{N_b^k} (s_{ij}^k - 1)^2, \quad (3)$$

i.e., as shown in Fig. 4, the sum of L2 loss between each element of the similarity matrix S and that of an all-one matrix. Denote the similarity loss of a batch of molecules as $\mathcal{L}_{sim} = \sum_{k=1}^N \mathcal{L}_{sim}^k$, then the loss for pre-training the FraSICL model is:

$$\mathcal{L} = \gamma \mathcal{L}_{sim} + \mathcal{L}_{clr}, \quad (4)$$

where γ is a hyper-parameter to adjust the influence of the auxiliary similarity loss.

3 Experiments

3.1 Baseline experiments

Experimental setting. To construct the pre-training dataset, 200K molecules are randomly sampled from the pre-training dataset of MolCLR, where 10 million molecules are gathered from the PubChem database [10]. The amount of pre-training data is generally smaller than that of the other baseline models, as shown in Tab. 2. 5% of the pre-training data are randomly selected as a validation set for model selection. 7 downstream tasks from MoleculeNet [31] are used as downstream target tasks for the baseline experiments. Scaffold splitting is used on each downstream task, with an 8 : 1 : 1 ratio for the training/validation/test sets.

When transferring a pre-trained FraSICL model to the target tasks, different strategies can be applied, including using which branch of the model for producing molecular representations, and whether to finetune the pre-trained model (PTM) on target tasks. In the baseline experiments, we adopt the more complex fragment view branch for molecular representations, and finetune the model together with prediction head on the target tasks.

Compared baseline models. Seven state-of-the-art self-supervised pre-training models for molecular representation learning are used as baseline models for comparison, including MolCLR [16], DMP [17], MEMO [18], GROVER [19], GraphLoG [21], PretrainGNNs [22] and KPGT [23]. The experimental results are shown in Tab. 3, where the data of baseline models are cited from the original papers of these models. The best score on each dataset is bold, and the second-best is underlined.

Table 2: The training details of the PTMs

PTM	Source of the pre-training dataset	Size
MolCLR	PubChem	10M
DMP	PubChem	10M
MEMO	GEOM-Drug	300K
GROVER	ZINC15 and ChEMBL	11M
GraphLoG	ZINC15	2M
PretrainGNNs	ZINC15 (self-supervised)	2M
	ChEMBL (supervised)	456K
KPGT	ChEMBL	2M
FraSICL	PubChem	200K

Results and analysis. As shown in Tab. 3, FraSICL achieves the best predictive performance on 5 of the 7 downstream MPP tasks, and the second on another one. As the number of pre-training samples used by FraSICL is only 200K, which is the least among these compared baseline models, the experimental results show that FraSICL can make better use of the information contained in the graph fragments of molecules to produce molecular representations with better predictive performance. Compared with the MEMO model that uses the same amount of pre-training data, the predictive performance of FraSICL on the 7 downstream tasks is significantly improved, even exceeds 20% on the BBBP dataset. And compared with the models such as GROVER and DMP-TF, FraSICL can achieve comparable or even higher predictive performance with only about 1/50 training samples. These results show the superiority of FraSICL to the existing models on molecular property prediction tasks.

Table 3: Results of performance comparison between FraSICL and major existing models on 7 downstream MPP tasks.

Model	BACE classification	BBBP classification	ClinTox classification	Tox21 classification	ESOL regression	FreeSolv regression	Lipop regression
MolCLR	0.890 ± 0.003	0.736 ± 0.005	0.932 ± 0.017	0.798 ± 0.007	1.110 ± 0.010	2.200 ± 0.200	0.650 ± 0.080
DMP-TF	0.893 ± 0.009	0.781 ± 0.005	0.950 ± 0.005	0.788 ± 0.005	0.700 ± 0.084	-	-
MEMO	0.826 ± 0.003	0.716 ± 0.010	0.816 ± 0.037	0.767 ± 0.004	0.984 ± 0.034	-	0.707 ± 0.001
GROVER	0.894 ± 0.028	0.940 ± 0.019	0.944 ± 0.021	0.831 ± 0.025	0.831 ± 0.120	1.544 ± 0.397	0.560 ± 0.035
PretrainGNNs	0.845 ± 0.007	0.687 ± 0.013	0.726 ± 0.015	0.781 ± 0.006	-	-	-
GraphLoG	0.835 ± 0.012	0.725 ± 0.008	0.767 ± 0.033	0.757 ± 0.005	-	-	-
KPGT	0.855 ± 0.011	0.908 ± 0.010	0.946 ± 0.022	0.848 ± 0.013	0.803 ± 0.008	2.121 ± 0.837	0.600 ± 0.010
FraSICL	0.896 ± 0.010	0.948 ± 0.003	0.957 ± 0.011	0.807 ± 0.006	0.626 ± 0.008	1.094 ± 0.027	0.581 ± 0.013

3.2 Experiments with different transferring settings

Experimental setting. In the baseline experiments, we choose finetuning the more complex and predictive fragment view branch as the transferring setting. In this section, other transferring settings are tested, i.e., the combinations of different branches and different fine-tuning strategies. Experiments are carried out on the BBBP, ClinTox, ESOL and FreeSolv datasets. Four transferring settings are evaluated, which are denoted as FraSICL-ft-mol, FraSICL-ft-frag, FraSICL-fr-mol, FraSICL-fr-frag, where *ft* represents finetuning the PTM, *fr* represents freezing the PTM, *mol* indicates using molecule views and *frag* indicates using fragment views.

Results and analysis. The experimental results are shown in Tab. 4. Since the two branches of FraSICL are asymmetric, the structure of the fragment view branch is more complex and has stronger learning capability. Thus, as is revealed by the experimental results, FraSICL-ft-frag achieves the best performance on 3 of the 4 target tasks. However, a more complex model structure indicates that it is more likely to suffer overfitting on the downstream tasks. So, when transferring to the FreeSolv dataset with only 642 samples, the performance of FraSICL-ft-frag is slightly inferior to that of FraSICL-ft-mol. In addition, compared with freezing the pre-trained model, finetuning model allows the PTM to obtain information about specific molecular properties from the supervised loss, thereby the generated molecular representations are more relevant to the target task. Thus a large improvement on the performance is achieved.

Table 4: Predictive performance of 4 FraSICL model variants with different transferring settings on 4 MPP tasks.

Model	BBBP classification	ClinTox classification	ESOL regression	FreeSolv regression
FraSICL-fr-mol	0.852 ± 0.003	0.691 ± 0.007	1.321 ± 0.002	2.548 ± 0.006
FraSICL-fr-frag	0.803 ± 0.010	0.628 ± 0.020	1.594 ± 0.217	2.293 ± 0.009
FraSICL-ft-mol	0.917 ± 0.006	0.906 ± 0.023	0.758 ± 0.029	1.085 ± 0.059
FraSICL-ft-frag	0.948 ± 0.003	0.957 ± 0.011	0.626 ± 0.008	1.094 ± 0.027

3.3 Influence of the auxiliary similarity loss

Motivation. The auxiliary similarity loss, i.e., Equ. (3) introduced in Sec. 2.5, is designed for making the fragment-pair views to learn from each other to better leverage the information encoded in different fragment-pair views. However, it is intuitive that when the auxiliary loss takes an excessively dominant role in the total training loss, the model may tend to generate exactly the same representation vectors for different fragment-pair views to decrease the similarity loss. On this occasion, the representation vectors of fragment-pair views will not contain any information about the topological structure, showing a model collapse phenomenon. Thus, the influence of the hyperparameter γ is crucial.

Experimental setting. In this section, experiments are conducted to test the influence of the auxiliary similarity loss by setting different γ . In these experiments, γ is set to 0.1, 0.01, 0.005 and 0 respectively, where $\gamma = 0$ indicates training without the similarity loss, which can be regarded as an ablation study. Here, the transferring setting is the same as the baseline experiments, i.e., finetuning the fragment view branch.

Results and analysis. Results are shown in Tab. 5. As shown in Tab. 5, the auxiliary similarity loss has an obvious impact on the predictive performance. When $\gamma = 0$, i.e., training without the similarity loss, the predictive performance is not superior to that of the other three models trained with the auxiliary similarity loss, which demonstrates that the auxiliary similarity loss can indeed promote the model to produce more predictive representations. And when $\gamma = 0.1$, the model achieves even worse results than $\gamma = 0$ on 3 of the 4 downstream tasks, which reveals that a large value of γ may make the similarity loss be harmful to the model and lead to performance degradation.

Table 5: Experimental results on the influence of hyperparameter γ .

γ	BBBP classification	ClinTox classification	ESOL regression	FreeSolv regression
0.1	0.890 \pm 0.023	0.916 \pm 0.008	0.734 \pm 0.028	1.151 \pm 0.098
0.01	0.948 \pm 0.003	0.957 \pm 0.011	0.626 \pm 0.008	1.094 \pm 0.027
0.005	0.927 \pm 0.008	0.912 \pm 0.012	0.667 \pm 0.024	1.148 \pm 0.015
0	0.906 \pm 0.009	0.880 \pm 0.030	0.662 \pm 0.051	1.138 \pm 0.092

4 Conclusion

This paper focuses on the semantic inconsistency problem that may occur when using noise-adding operations to generate new views for contrastive learning in self-supervised molecular property prediction studies. To solve this problem, this paper first defines semantic-invariant molecular view by introducing two types of semantic inconsistent views that may lead to false positive pairs and consequently poor performance. Then, a semantic-invariant view generation method is proposed. The views generated by this method will not cause semantic inconsistency, which realizes the decoupling of the input graph topology and the message passing topology of GNNs. Thus, this method is expected to promote the GNN encoders to extract better molecular representations.

Based on the semantic-invariant views, a Fragment-based Semantic-Invariant Contrastive Learning (FraSICL) molecular representation model is developed. FraSICL is an asymmetric model with two branches, the molecule view branch and the fragment view branch. A multi-view fusion mechanism is also introduced to make better use of the information contained in the views of different fragment pairs. Furthermore, an auxiliary similarity loss is designed to train the backbone GNN to produce better representations.

Baseline experiments are conducted on 7 target tasks, and experimental results show that FraSICL achieves state-of-the-art predictive performance with the least number of pre-training data. Further experiments demonstrate that in our model finetuning is effective in boosting performance and the auxiliary similarity loss can improve the predictive accuracy if a proper hyperparameter γ is selected. These findings reveal that FraSICL can make better use of the information of pre-training samples and generate representations with superior predictive performance.

References

- [1] Justin Gilmer, Samuel S Schoenholz, Patrick F Riley, Oriol Vinyals, and George E Dahl. Neural message passing for quantum chemistry. In *Proceedings of the 34th International Conference on Machine Learning (ICML)*, volume 70, pages 1263–1272. PMLR, 2017.
- [2] David K Duvenaud, Dougal Maclaurin, Jorge Iparraguirre, Rafael Bombarell, Timothy Hirzel, Alán Aspuru-Guzik, and Ryan P Adams. Convolutional networks on graphs for learning molecular fingerprints. In *Advances in Neural Information Processing Systems*, volume 28, pages 2224–2232, 2015.
- [3] Sabrina Jaeger, Simone Fulle, and Samo Turk. Mol2vec: unsupervised machine learning approach with chemical intuition. *Journal of chemical information and modeling*, 58(1):27–35, 2018.
- [4] Ying Song, Shuangjia Zheng, Zhangming Niu, Zhang-Hua Fu, Yutong Lu, and Yuedong Yang. Communicative representation learning on attributed molecular graphs. In *Proceedings of the Twenty-Ninth International Joint Conference on Artificial Intelligence*, pages 2831–2838, 2020.
- [5] Zhaoping Xiong, Dingyan Wang, Xiaohong Liu, Feisheng Zhong, Xiaozhe Wan, Xutong Li, Zhaojun Li, Xiaomin Luo, Kaixian Chen, Hualiang Jiang, et al. Pushing the boundaries of molecular representation for drug discovery with the graph attention mechanism. *Journal of medicinal chemistry*, 63(16):8749–8760, 2019.
- [6] Ziqiao Zhang, Jihong Guan, and Shuigeng Zhou. Fragat: a fragment-oriented multi-scale graph attention model for molecular property prediction. *Bioinformatics*, 37(18):2981–2987, 2021.
- [7] Chengxuan Ying, Tianle Cai, Shengjie Luo, Shuxin Zheng, Guolin Ke, Di He, Yanming Shen, and Tie-Yan Liu. Do transformers really perform badly for graph representation? In *Advances in Neural Information Processing Systems*, volume 34, pages 28877–28888, 2021.
- [8] Han Altae-Tran, Bharath Ramsundar, Aneesh S Pappu, and Vijay Pande. Low data drug discovery with one-shot learning. *ACS central science*, 3(4):283–293, 2017.

- [9] Anna Gaulton, Anne Hersey, Michał Nowotka, A Patricia Bento, Jon Chambers, David Mendez, Prudence Mutowo, Francis Atkinson, Louisa J Bellis, Elena Cibrián-Uhalte, et al. The chembl database in 2017. *Nucleic acids research*, 45(D1):D945–D954, 2017.
- [10] Sunghwan Kim, Jie Chen, Tiejun Cheng, Asta Gindulyte, Jia He, Siqian He, Qingliang Li, Benjamin A Shoemaker, Paul A Thiessen, Bo Yu, Leonid Zaslavsky, Jian Zhang, and Evan E Bolton. PubChem in 2021: new data content and improved web interfaces. *Nucleic Acids Research*, 49(D1):D1388–D1395, 2021.
- [11] John J. Irwin, Khanh G. Tang, Jennifer Young, Chinzorig Dandarchuluun, Benjamin R. Wong, Munkhzul Khurelbaatar, Yurii S. Moroz, John Mayfield, and Roger A. Sayle. Zinc20—a free ultralarge-scale chemical database for ligand discovery. *Journal of Chemical Information and Modeling*, 60(12):6065–6073, 2020.
- [12] Jacob Devlin, Ming-Wei Chang, Kenton Lee, and Kristina Toutanova. Bert: Pre-training of deep bidirectional transformers for language understanding. In *Proceedings of the 2019 Conference of the North American Chapter of the Association for Computational Linguistics: Human Language Technologies (NAACL-HLT)*, volume 1, pages 4171–4186. Association for Computational Linguistics, 2019.
- [13] Kaiming He, Haoqi Fan, Yuxin Wu, Saining Xie, and Ross Girshick. Momentum contrast for unsupervised visual representation learning. In *Proceedings of the IEEE/CVF Conference on Computer Vision and Pattern Recognition (CVPR)*, pages 9726–9735. CVF/IEEE, 2020.
- [14] Ting Chen, Simon Kornblith, Mohammad Norouzi, and Geoffrey Hinton. A simple framework for contrastive learning of visual representations. In *Proceedings of the 37th International Conference on Machine Learning (ICML)*, volume 119, pages 1597–1607. PMLR, 2020.
- [15] Ashish Jaiswal, Ashwin Ramesh Babu, Mohammad Zaki Zadeh, Debapriya Banerjee, and Fillia Makedon. A survey on contrastive self-supervised learning. *Technologies*, 9(1):2, 2020.
- [16] Yuyang Wang, Jianren Wang, Zhonglin Cao, and Amir Barati Farimani. Molecular contrastive learning of representations via graph neural networks. *Nature Machine Intelligence*, 4(3):279–287, 2022.
- [17] Jinhua Zhu, Yingce Xia, Tao Qin, Wengang Zhou, Houqiang Li, and Tie-Yan Liu. Dual-view molecule pre-training. *CoRR*, abs/2106.10234, 2021.
- [18] Yanqiao Zhu, Dingshuo Chen, Yuanqi Du, Yingze Wang, Qiang Liu, and Shu Wu. Featurizations matter: A multiview contrastive learning approach to molecular pretraining. In *ICML 2022 2nd AI for Science Workshop*, 2022.
- [19] Yu Rong, Yatao Bian, Tingyang Xu, Weiyang Xie, Ying Wei, Wenbing Huang, and Junzhou Huang. Self-supervised graph transformer on large-scale molecular data. In *Advances in Neural Information Processing Systems*, volume 33, pages 12559–12571, 2020.
- [20] Hyunseob Kim, Jeongcheol Lee, Sunil Ahn, and Jongsuk Ruth Lee. A merged molecular representation learning for molecular properties prediction with a web-based service. *Scientific Reports*, 11(1):1–9, 2021.
- [21] Minghao Xu, Hang Wang, Bingbing Ni, Hongyu Guo, and Jian Tang. Self-supervised graph-level representation learning with local and global structure. In *Proceedings of the 38th International Conference on Machine Learning (ICML)*, volume 139, pages 11548–11558. PMLR, 2021.
- [22] Weihua Hu, Bowen Liu, Joseph Gomes, Marinka Zitnik, Percy Liang, Vijay Pande, and Jure Leskovec. Strategies for pre-training graph neural networks. In *8th International Conference on Learning Representations, ICLR*, 2020.
- [23] Han Li, Dan Zhao, and Jianyang Zeng. Kpqt: Knowledge-guided pre-training of graph transformer for molecular property prediction. *arXiv preprint arXiv:2206.03364*, 2022.
- [24] David Rogers and Mathew Hahn. Extended-connectivity fingerprints. *Journal of chemical information and modeling*, 50(5):742–754, 2010.
- [25] David Weininger. Smiles, a chemical language and information system. 1. introduction to methodology and encoding rules. *Journal of Chemical Information and Computer Sciences*, 28(1):31–36, 1988.
- [26] Henri A Favre and Warren H Powell. *Nomenclature of Organic Chemistry*. The Royal Society of Chemistry, 2014.
- [27] Jean-Bastien Grill, Florian Strub, Florent Altché, Corentin Tallec, Pierre Richemond, Elena Buchatskaya, Carl Doersch, Bernardo Avila Pires, Zhaohan Guo, Mohammad Gheshlaghi Azar, et al. Bootstrap your own latent—a new approach to self-supervised learning. *Advances in neural information processing systems*, 33:21271–21284, 2020.
- [28] Jake Topping, Francesco Di Giovanni, Benjamin Paul Chamberlain, Xiaowen Dong, and Michael M Bronstein. Understanding over-squashing and bottlenecks on graphs via curvature. In *10th International Conference on Learning Representations, ICLR*, 2022.

- [29] Uri Alon and Eran Yahav. On the bottleneck of graph neural networks and its practical implications. In *9th International Conference on Learning Representations, ICLR, 2021*.
- [30] Rickard Brüel-Gabrielsson, Mikhail Yurochkin, and Justin Solomon. Rewiring with positional encodings for graph neural networks. *arXiv preprint arXiv:2201.12674*, 2022.
- [31] Zhenqin Wu, Bharath Ramsundar, Evan N Feinberg, Joseph Gomes, Caleb Geniesse, Aneesh S Pappu, Karl Leswing, and Vijay Pande. Moleculenet: a benchmark for molecular machine learning. *Chemical science*, 9(2):513–530, 2018.